Pergamon

Bioorganic & Medicinal Chemistry 10 (2002) 3619–3625

BIOORGANIC & MEDICINAL CHEMISTRY

Thalassiolins A–C: New Marine-Derived Inhibitors of HIV cDNA Integrase

David C. Rowley,[a,*] Mark S. T. Hansen,[b] Denise Rhodes,[b] Christoph A. Sotriffer,[c] Haihong Ni,[c] J. Andrew McCammon,[c] Frederic D. Bushman[b] and William Fenical[a]

[a]*Center for Marine Biotechnology and Biomedicine, Scripps Institution of Oceanography, University of California–San Diego, La Jolla, CA 92093, USA*

[b]*Infectious Disease Laboratory, The Salk Institute, 10010 North Torrey Pines Road, La Jolla, CA 92037, USA*

[c]*Department of Chemistry and Biochemistry, Department of Pharmacology, University of California–San Diego, La Jolla, CA,92093, USA*

Received 31 January 2002; accepted 29 April 2002

Abstract—Human immunodeficiency virus (HIV) replication requires integration of viral cDNA into the host genome, a process mediated by the viral enzyme integrase. We describe a new series of HIV integrase inhibitors, thalassiolins A–C (**1**–**3**), isolated from the Caribbean sea grass *Thalassia testudinum*. The thalassiolins are distinguished from other flavones previously studied by the substitution of a sulfated β-D-glucose at the 7-position, a substituent that imparts increased potency against integrase in biochemical assays. The most active of these molecules, thalassiolin A (**1**), displays in vitro inhibition of the integrase catalyzed strand transfer reaction ($IC_{50} = 0.4$ μM) and an antiviral IC_{50} of 30 μM. Molecular modeling studies indicate a favorable binding mode is probable at the catalytic core domain of HIV-1 integrase.

Introduction

Highly active antiretroviral therapy using reverse transcriptase and protease inhibitors has been successful in suppressing viremia to undetectable levels in some HIV patients. However, new antiretroviral drugs, especially those with novel modes of action, are required to address rapidly developing viral resistance. Integrase is an essential enzyme in the replication cycle of HIV, and represents an attractive drug target since it shares no functional homology with normal cellular proteins.[1,2] However, the development of a clinically useful integrase inhibitor remains an elusive goal.

The viral-encoded integrase enzyme carries out the covalent integration of the double stranded cDNA product of reverse transcription into a chromosome of the host cell (Fig. 1A). After binding to the viral cDNA, integrase mediates endonucleolytic processing to cleave a dinucleotide from each 3′ end. The 3′-hydroxyls groups exposed by this cleavage step are then joined to 5′ ends in the target DNA in a single step transesterification reaction. The points of covalent joining in the target DNA are separated by five base pairs. Subsequent melting of these base pairs followed by DNA repair completes the formation of the provirus.[1,2]

The development of in vitro assays based on this model has aided in the identification of small molecule integrase inhibitors. Typically, purified integrase is used to catalyze the reactions of 3′-processing and strand transfer on oligonucleotides matching one end of the unintegrated HIV cDNA (Fig. 1B). Several studies have emphasized the importance of studying correctly assembled integrase complexes, because these display a response to inhibitors not recaptulated in simpler assays.[3–5]

Using tests against such preassembled complexes, workers at Merck have reported a series of diketo acids that display specific and potent in vitro inhibition of integrase, as well as antiviral activity against HIV in cell culture.[5,6] HIV-1 variants resistant to these compounds consistently contained specific mutations in the integrase coding region, documenting action against integrase in vivo. Other reported integrase inhibitors have either lacked antiviral efficacy, suffered from toxicity problems, or have been proven to block viral replication

*Corresponding author at current address: Department of Biomedical Sciences, College of Pharmacy, University of Rhode Island, 41 Lower College Road, Kingston, RI 02881, USA. Tel.: +1-401-874-9228; fax: +1-401-874-5048; e-mail: drowley@uri.edu

0968-0896/02/$ - see front matter © 2002 Elsevier Science Ltd. All rights reserved.
PII: S0968-0896(02)00241-9

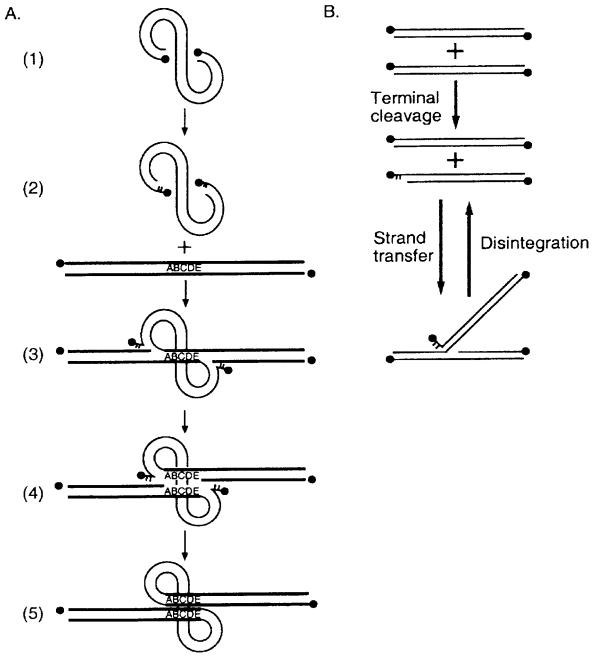

Figure 1. DNA processing events mediated by HIV Integrase. (A) Viral cDNA from reverse transcription (1) is processed by cleavage of two nucleotides from 3′ end (2). The recessed 3′ ends are then joined to protruding 5′ strand breaks in the host DNA (3). The points of joining of the two DNA molecules are offset by five base pairs, A–E, that subsequently melt (4). Filling and sealing of these gaps then yields the integrated provirus (5). (B) Assay reactions catalyzed in vitro by purified integrase.

steps other than DNA integration in vivo.[7] Nevertheless, the in vitro activities of these clinically non-useful inhibitors add to a growing body of structure–activity relationship data that may prove useful in the future design of integrase inhibitors.

Our aim has been the identification of new small molecule inhibitors of HIV integrase derived from unique marine sources. We have used assays with preasssembled complexes as described[8] to screen a set of extracts of marine organisms. Here we describe the HIV integrase inhibitory properties of the thalassiolins A–C, a series of water-soluble flavones isolated from the Caribbean sea grass *Thalassia testudinum* (Fig. 2). The thalassiolins contain unique functionality in the form of β-D-glucopyranosyl-2″-sulfate, a substituent that imparts increased potency against integrase in biochemical assays versus the parent flavone. Thalassiolin A (**1**) displays submicromolar in vitro activity against the strand transfer reaction, inhibits HIV replication in cell culture, and is relatively non-cytotoxic. To gain insight into the potential binding modes of these inhibitors, molecular docking simulations probing how these compounds might interact with the catalytic core domain of HIV-1 integrase have been conducted.

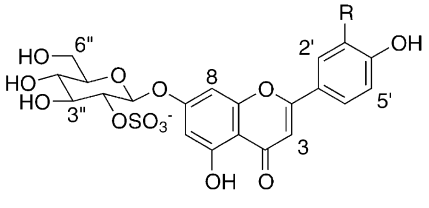

1 R = OH
2 R = OMe
3 R = H

Figure 2. Structures of the thalassiolins isolated from *T. testudinum*.

Results

Isolation and characterization of thalassiolins A–C

Thalassia testudinum was collected from a shallow lagoon located at Little San Salvador Island in the Bahamas. The sea grass was blended with deionized H_2O and then filtered through Celite to remove particulates. The filtrate was vacuum filtered through C18 silica gel, and the active components retained on the resin were eluted with 10% MeCN in H_2O. The lyophilized fraction was further separated by size exclusion chromatography (LH-20, MeOH), followed by C18 reversed phase HPLC (5→15% MeCN in H_2O, 30 min) to provide pure thalassiolins A–C (**1**–**3**).

Thalassiolin A (**1**) was identified as luteolin 7-β-D-glucopyranosyl-2″-sulfate by comparison of ^1H and ^{13}C NMR, IR, and mass spectral data with the previously reported compound.[9] This molecule had been implicated in the chemical defense of the seagrass against pathogenic marine microorganisms. The ^1H and ^{13}C NMR data for thalassiolin B (**2**) (Table 1) largely resembled those of thalassiolin A. High resolution MALDI FTMS data established a molecular formula $C_{22}H_{21}O_{14}S$ for thalassiolin B, suggesting the difference between **1** and **2** was the presence of an additional methyl group. This was supported by the presence of a singlet in the ^1H NMR spectrum at 3.89 ppm that integrated for three protons, and an additional ^{13}C NMR signal at 56.0 ppm that the DEPT spectrum indicated to be a methyl carbon. The downfield position of these resonances was consistent with the methyl group attached to oxygen. A strong HMBC correlation between this methyl carbon was observed to C-3′, establishing its position on the phenyl ring (Fig. 3). Comprehensive NMR data allowed all other protons and carbons to be assigned, leading to the assignment of the planar structure, **2**, for thalassiolin B.

Thalassiolin C (**3**) analyzed for the molecular formula $C_{21}H_{19}O_{13}S$ by high resolution MALDI FTMS, a difference of one oxygen atom from that of **1**. A *para*-

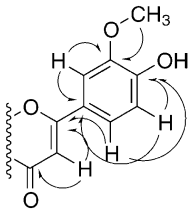

Figure 3. Partial HMBC analysis of thalassiolin B (**2**).

Table 1. ^{1}H and ^{13}C NMR Assignments for Thalassiolins A–C in DMSO-d_6

Compd	Thalassiolin A (**1**)		Thalassiolin B (**2**)		Thalassiolin C (**3**)	
	^{13}C[a]	^{1}H[b] [m, *J* (Hz)]	^{13}C	^{1}H [m, *J* (Hz)]	^{13}C	^{1}H [m, *J* (Hz)]
2	164.6		164.3		164.4	
3	102.9	6.75 (s)	103.2	6.96 (s)	102.6	6.82 (s)
4	181.9		182.0		181.9	
5	161.2		161.2		161.2	
6	99.6	6.42 (s)	99.4	6.42 (s)	99.5	6.39 (s)
7	162.7		162.6		162.6	
8	95.0	6.76 (s)	95.3	6.82 (d, 1.8)	95.0	6.78 (d, 1.8)
9	156.9		156.9		156.8	
10	105.4		105.4		105.4	
1′	120.8		120.8		119	
2′	113.3	7.44 (s)	110.1	7.58 (s)	128.7	7.92 (d, 8.7)
3′	146.0		148.2		116.3	6.87 (d, 8.4)
4′	150.7		151		162.6	
5′	116.0	6.89 (d, 8.1)	115.9	6.92 (d, 8.5)	116.3	6.87 (d, 8.4)
6′	119.3	7.46 (dd, 8.1, 1.5)	120.7	7.60 (dd, 8.5, 1.2)	128.7	7.92 (d, 8.7)
1″	97.4	5.30 (d, 7.5)	97.3	5.28 (d, 7.8)	97.2	5.3 (d, 7.8)
2″	78.5	4.04 (dd, 7.8)	78.5	4.03 (dd, 8.1)	78.4	4.02 (dd, 8.4)
3″	75.9	3.62 (dd, 8.7)	75.9	3.61 (dd, 8.7)	75.9	3.60 (dd, 8.4)
4″	69.4	3.28 (dd, 9)	69.5	3.26 (dd, 9)	69.4	3.28 (m)
5″	76.9	3.52 (m)	76.9	3.50 (m)	76.8	3.50 (m)
6″	60.5	3.73 (m)	60.5	3.71 (d, 9.9)	60.4	3.70 (m)
		3.49 (dd, 10.2)		3.49 (m)		3.48 (m)
OMe			56.0	3.89 (s)		

[a]100 MHz.
[b]300 MHz Assignments by DEPT, COSY, HMQC, and HMBC.

substituted phenol was easily recognized by symmetry in both the ^{13}C NMR spectrum and the ^{1}H NMR aromatic proton coupling pattern (Table 1). Hence, substitution of a phenol for the catechol ring of **1** accounts for the one less oxygen. All 2D-NMR data, including COSY, gHMQC, and gHMBC, were consistent with these assignments. Proton and ^{13}C chemical shift and coupling constant data, as well as IR data, fully supported the sugar moieties of **2** and **3** as matching that of **1**. Compounds **2** and **3** were therefore identified as chrysoeriol 7-β-D-glucopyranosyl-2″-sulfate and apigenin 7-β-D-glucopyranosyl-2″-sulfate, respectively.

Biological properties of the thalassiolins A–C

IC_{50} values for inhibition of purified HIV integrase protein were determined using two assays. In the first, purified integrase was incubated with end-labeled DNA substrates and various concentrations of **1**–**3**. Reaction products were denatured and separated by electrophoresis on denaturing polyacrylamide gels. Reactions were quantitated by phosphorimager analysis of the radioactive products.[10–13] These reactions were carried out in the presence of Mn^{+2} as the metal cofactor.

Thalassiolin A was most active, inhibiting the integrase terminal cleavage and strand transfer activities with IC_{50} values of 2.1 and 0.4 μM, respectively (Fig. 4 and Table 2). Thalassiolins B and C were less potent inhibitors, with IC_{50} values in the 30–100 μM range.

Inhibitory activities against the strand transfer reaction were compared in the presence of Mg^{+2}, since this is more likely to be the metal cofactor utilized in vivo. Integrase was preassembled with viral DNA substrates

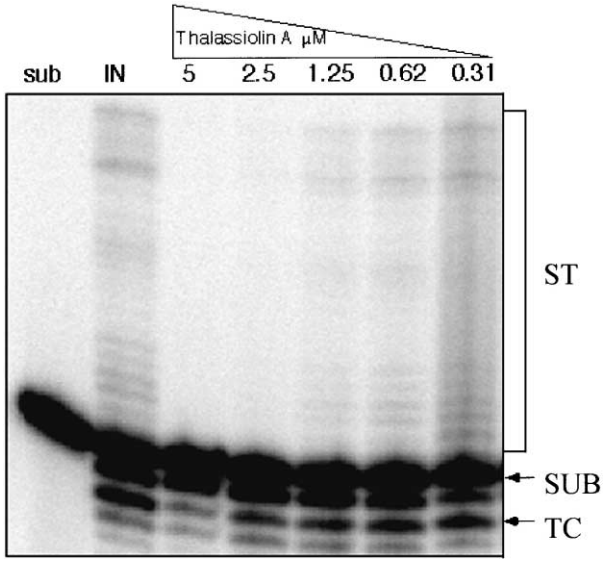

Figure 4. Inhibition of integration in vitro by thalassiolin A. The figure displays an autoradiogram of reaction products. The lane marked 'sub' contained only substrate; the others contained full length HIV-1 integrase. The concentrations of thalassiolin A tested are indicated above the lanes. The mobility of the substrate (SUB), terminal cleavage (TC), and strand transfer (ST) products are marked with arrows. Thalassiolin A inhibited terminal cleavage and strand transfer reactions with IC_{50} values of 2.1 and 0.4 μM, respectively.

in these assays, thereby mimicking the stably assembled preintegration complexes active in vivo, as described by Hwang and co-workers.[8] Hazuda and co-workers have reported that screens using such preassembled complexes can yield inhibitors active against HIV in cell culture.[5] Thalassiolin A inhibited the Mg^{+2} dependent strand transfer reaction with an IC_{50} of 2 μM. Thalassiolins B and C were inactive in this assay.

Table 2. IC_{50} inhibitory activities of the thalassiolins (μM)

Compd	Purified integrase		ELISA[b]	Live virus	LD_{50}[d]	MCV Topo
	T. Cl.[a]	Str. Tr.[a]				
Thalassiolin A (**1**)	2.1	0.4	2	27	>800	>200
Thalassiolin B (**2**)	112	43	>200	ND[c]	>800	>200
Thalassiolin C (**3**)	67	28	140	ND[c]	>800	>200

[a]Mn^{2+} metal cofactor.
[b]Mg^{2+} metal cofactor.
[c]ND = not done.
[d]Cytotoxicity against MT2 cells.

The antiviral activity of thalassiolin A against HIV replication was determined using the MAGI indicator cell assay in which infected centers score as β-galactosidase positive syncytia.[14] The addition of **1** to infected cultures inhibited infection with an IC_{50} of about 30 μM. Since the MAGI assay requires HIV to complete cell entry, reverse transcription, integration, and gene expression, we can deduce that the step affected by thalassiolin A is one of these.

The effect of **1** on the growth of HIV over multiple cycles of viral replication was also assessed (Fig. 5). Cultures were infected with low titers of HIV and viral replication monitored by assaying synthesis of the viral capsid protein p24. HIV overgrew the culture within 10 days, while in the presence of **1** growth was barely detectable. Taken together, these studies document inhibition of HIV replication by thalassiolin A.

As a test of the specificity of inhibition, the effects of **1**–**3** were tested against the topoisomerase of the pathogenic poxvirus MCV (molluscum contagiosum virus) (Table 2). Assays monitored the strand cleavage and religation activities of this enzyme.[15] The IC_{50} values were found to be greater than 200 μM, the highest concentration tested.

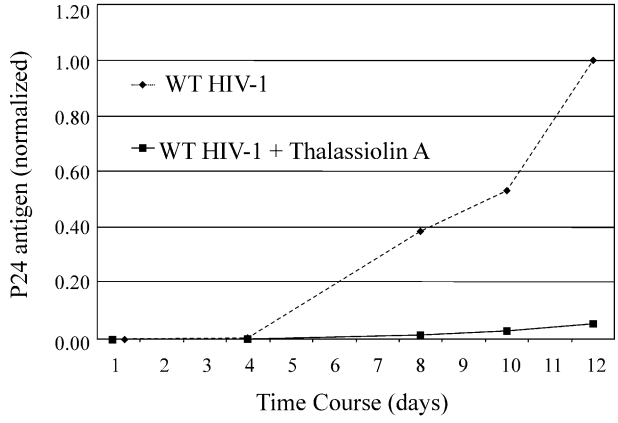

Figure 5. Response of HIV-1 replication to 300 μM thalassiolin A in a multi-cycle replication assay. MT-2 cells were inoculated with 2 ng p24 in a volume of 5 mL at 2×10^5 cells per mL. Cells were inoculated with virus in the absense or presence of 300 μM thalassiolin A. P24 antigen in the supernatant was monitored over an 11-day time course. Fresh media and drug was added every 48 h and cells were maintained between 2×10^5 and 8×10^5 per mL. Values are normalized to the maximal value.

Cellular toxicity was also monitored. No toxicity was detected against MT2 cells at 800 μM, the highest concentration tested. Similarly, no toxicity was observed against HCT-116 cells at 75 μM.

It is uncertain whether the step affected by **1** in vivo is indeed integration. The above data is consistent with this, but we note that previous studies have found that compounds of this class may also affect viral entry. Attempts to obtain virus that are resistant to **1** by long term passage of HIV in the presence **1** have so far not been successful (data not shown). Further studies are needed to clarify possible activity against integrase in vivo.

Possible binding sites of the thalassiolins on integrase

Several studies have identified the probable catalytic site of HIV integrase, and established that three acidic resudues Asp-64, Asp-116, and Glu-152 are required for function.[16,17] Goldgur et al. have described a crystal structure of the integrase inhibitor 5CITEP complexed in the active site.[18] Molecular modeling techniques have been successful in reproducing the experimental binding mode of this inhibitor, and should therefore be useful in analyzing possible binding modes other HIV-1 integrase inhibitors as well.[19]

Docking of thalassiolin A to the active site revealed a favorable binding site close to the catalytic center (Fig. 6). For the top-ranked result of the computational search, a free energy of binding of −7.2 kcal/mol is calculated. In this energetically preferred binding mode, the sulfated glucose ring is embedded in a shallow pocket surrounded by His 67, Lys 156, and Lys 159. At the bottom of this pocket it interacts with Cys 65, Thr 66, and Asn 155. The 6″-oxygen is coordinated to the Mg^{+2} ion, and the sulfate interacts with the two lysine side chains (Lys 156, Lys 159). The benzopyranone ring is placed close to Gln 148 and Glu 152, while the catechol ring extends into the space between Gln 148 and Asp 116, showing additional interactions with Asn 117 and the backbone of Phe 139.

The computer-based docking result also revealed a variant of this possible binding mode. It shows a somewhat less favorable free energy of binding (−7.0 kcal/mol), but needs to be considered as a possible alternative. While the glucose and sulfate are similarly oriented as in

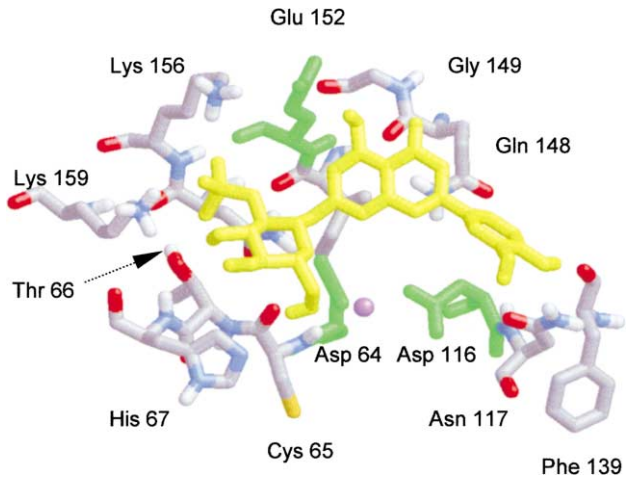

Figure 6. Computer-generated docking of thalassiolin A to the catalytic core domain of HIV-1 integrase. The inhibitor is shown in yellow and the catalytic residues (64, 116, 152) are highlighted in green, while the other amino acids are color coded by atom type; the metal ion is shown in violet. Except for the buried residues Ile 151 and Asn 155, all displayed amino acids are labeled.

the first result, the position of the catechol ring and the orientation of the benzopyranone system are different. The catechol is now found in a rather exposed position between Gly 149 and Glu 152. The benzopyranone, instead, occupies exactly the same plane as in the first binding mode, but rotated by 180° such that the hydroxy group (5-OH) points to Asp 116 instead of Glu 152.

Docking of **2** and **3** to the active site provided essentially the same binding modes as observed for **1**, but with slightly less favorable binding free energy (−6.2 to −6.8 kcal/mol) for the least strained conformations, consistent with the possibility that this is a biologically relevant binding mode.

Discussion

The HIV integrase inhibitory properties of the thalassiolins A–C, a series of sulfated-flavone glycosides isolated from the Caribbean sea grass *Thalassia testudinum*, were identified during a screening effort involving several thousand of marine extracts from diverse sources. The lead compound thalassiolin A (**1**) showed inhibition of reactions catalyzed by purified integrase in addition to antiviral activity against HIV in cell culture. The thalassiolins are non-cytotoxic, water soluble, and relatively easy to acquire, making them interesting candidates for further study as anti-HIV agents.

Polyhydroxylated aromatic compounds have been previously identified as inhibitors of HIV integrase. Activity is generally correlated to the presence of at least one pair of vicinal hydroxyl groups on an aromatic ring. Examples include quinalizarin,[4] flavones such as quercetin,[20] and the bis-catechols α-conidendrin and hematoxylin.[21] A shortcoming of these inhibitors is that in vitro enzyme inhibition has generally not translated to antiviral activity. An exception to this trend is L-chicoric acid, although this bis-catechol has recently been demonstrated to block viral entry as a primary mode of action.[7] Sulfated phenols have also been previously reported as in vitro inhibitors of HIV integrase. Lamellarin-α-20-sulfate shows moderate activity against purified enzyme and PICs, as well as more potent antiviral activity against HIV.[22] Suramin,[23] naphthalenesulfonic acid derivatives,[24] and sulfonated biphenyls[25] are further examples. However, the presence of a sulfated sugar alone is not sufficient to impart in vitro inhibitory properties against HIV integrase.[24]

Compound **1** is unusually potent against integrase compared with previously studied flavones, due at least in part to the modified sugar resisdue attached to the flavone moiety. In contrast to our results, glycosylation of flavones has been reported to reduce or eliminate integrase activity. In the case of quercetin, substitutions at the 3-position with rhamnose, arabinose, glucose, or rutinose lead to significantly less potent or inactive compounds. Substitution of glucose at position 8 diminished the potency by a factor of 2–3.[26] One apparent exception to the glycosylation trend are naturally occurring quercetin glycosides with either one or two gallate esters appended to a galactose at the flavone 3-position.[27] Thalassiolin A is more potent, and to our knowledge the only glycosylated flavone reported that is more active than the parent aglycone. Although sugar substitution at the 7-position has not been well studied, methylation of quercetrin at this site has been shown to decrease integrase activity by approximately 2-fold.[26] Perhaps then it is an appropriately placed sulfate that is responsible for the increased activity of these inhibitors.

Computational docking studies can help to generate hypotheses about protein–inhibitor interactions. The docking method used here has been shown to reproduce the experimental binding mode of the IN-inhibitor 5CITEP[18] visualized by crystallography.[19] We have therefore employed this tool to examine possible binding modes of **1**. The results suggest that the thalassiolins can be accommodated near the catalytic center. Interestingly, the binding modes overlap with the location of 5CITEP determined experimentally.[18] The tetrazole ring of this inhibitor occupies the same binding position as the sulfated glucose of the thalassiolins, and the orientations of the keto-enol and chloroindole moieties of 5CITEP show similarities with the benzopyranone binding position. The apparent similarities in binding by these structurally different molecules could inform future designs of inhibitors binding to the integrase active site.

The estimated binding free energies of **1**–**3** compares well with the expected affinities based on the IC_{50} values. In both binding modes suggested for **1**, the catechol ring is fairly exposed and the 3′-OH forms a weak hydrogen bond (with the side chains of Asn 117 and Glu 152, respectively). However, the catechol ring is located in a protein region known to be flexible. Possibly local conformational changes occur which lead to better hydrogen bond geometry and an improved fit for the catechol ring. Consequently, the substitution of the 3′-OH (**1**) with a methoxy group (**2**) or a hydrogen atom (**3**) may have a more dramatic effect on the binding

energy than observed in the docking simulations, in which the protein is required to be rigid.

Although **1** clearly acts against preassembled integrase complexes in vitro, it is unclear whether **1** is active against integrase during infection in vivo. The catechol-containing compound L-chicoric acid was initially thought to inhibit integration in vivo,[28] but more recent data indicates that the viral envelope is the more likely target.[7] We have attempted to obtain virus resistant to **1** by prolonged culture in the presence of drug, but so far no resistant mutants have been obtained, leaving open the question of the in vivo target. Regardless of whether integrase is the target in vivo, compound **1** is nevertheless a potent inhibitor of preassembled integrase complexes in vitro and HIV in vivo, and so may be a starting point for drug development.

Experimental

Thalassiolin B (2)

Yellow amorphous solid; $[\alpha]_D = -72^\circ$ ($c = 0.25$, MeOH); IR (neat) 3378, 1659, 1602, 1497, 1259, 1073, 1029, 1001, 817; UV (MeOH) λ_{max} 346 (ε 20 600), 268 (ε 15 900), 251 (ε 16 800), 207 (ε 35 800); HRMALDI FTMS *m/z* 541.0636 $[M–H^+]^-$, calcd for $C_{22}H_{21}O_{14}S$, 541.0657 ($\Delta = 3.9$ ppm); ^1H and ^{13}C NMR data are shown in Table 1.

Thalassiolin C (3)

Yellow amorphous solid; $[\alpha]_D = -54^\circ$ ($c = 0.25$, MeOH); IR (neat) 3384, 1653, 1605, 1497, 1244, 1177, 1073, 1000, 835; UV (MeOH) λ_{max} 334 (ε 13 600), 268 (ε 12 300), 207 (ε 23 400); HRMALDI FTMS *m/z* 511.0552 $[M–H^+]^-$, calcd for $C_{21}H_{19}O_{13}S$, 511.0552 (Δ 0 ppm); ^1H and ^{13}C NMR data are shown in Table 1.

In vitro assays

Assays of purified HIV integrase were either carried out with Mn^{2+} as the metal cofactor and assayed on gels, or carried out with Mg^{2+} and assayed in microtiter plates.[8] HIV integrase was purified to apparent homogeneity essentially as described in Bushman et al.[29] In assays with Mg, integrase and LTR DNA were preassembled by pre-incubation as described.[8] Assays with such preassembled complexes have yielded inhibitors with antiviral activity in previous studies.[5] Assays of MCV topoisomerase were carried out using a microtiter assay that monitored religation of oligonucleotide substrates.[8] p24 ELISA (DuPont) was carried out according to the manufacturer's protocol.

Cell culture

MT-2 cells were maintained between 2×10^5 and 1×10^6 cells in RPMI (BioWhitaker) supplemented with 10% FCS (GIBCO). MT-2 cells producing HIV-1 strain R9 were grown in RPMI supplemented with 20% FCS. P4 Cells[30] were maintained in DMEM (BioWhitaker) supplemented with 10% FCS.

Infections

10^6 MT-2 cells were infected at a multiplicity of infection approximately equal to 0.01 (2 ng p24) in a 5 mL culture containing 8 μg/mL polybrene (Sigma). Parallel infections were carried out in the absence or presence of 300 μM thalassiolin A. Infected cells were maintained between 2×10^5 and 8×10^5 cells per mL. Samples were removed, filtered, and assayed for the presence of p24 antigen. P4 cells were plated in 96 well plates at 10^4 cells per well. The following day, growth media was aspirated and cells were infected with R9HIV-1 virus in the absence or presence of varying concentrations of **1**. Ten microlitres of viral supernatant was diluted to a volume of 100 μL in the presence or absence of thalassiolin A and incubated for 5 min at room temperature. Supernatants were applied to plate wells for 3 h at 37 °C. For detection of infected centers, reactions were incubated for 48 h, fixed with glutaraldehyde and paraformaldehyde for 30 min and stained with X-Gal. Infected centers in each well were counted (600 for uninhibited reactions) and plotted as a percentage of the uninhibited reaction.

Modeling of thalassiolins A–C in the active site

Docking was performed with version 3.0 of the program AutoDock using the new empirical free energy function to evaluate binding free energies and the Lamarckian genetic algorithm to search for favorable binding positions.[31] While the protein is required to be rigid, the program allows torsional flexibility in the ligand. A standard AutoDock protocol was applied, with an initial population of 50 randomly placed individuals, a maximum number of 3.0×10^6 energy evaluations, a mutation rate of 0.02, a crossover rate of 0.80, and an elitism value of 1. Proportional selection was used, where the average of the worst energy was calculated over a window of the previous 10 generations. For the local search the so-called pseudo-Solis and Wets algorithm was applied using a maximum of 300 iterations per local search. The probability of performing local search on an individual in the population was 0.06, and the maximum number of consecutive successes or failures before doubling or halving the local search step size was four. Fifty independent docking runs were carried out for each ligand using these parameters.

The structures of the ligands were generated with QUANTA® and optimized with the implemented CHARMm® force field (these programs are distributed by Molecular Simulations Incorporated). Atomic charges were assigned using the Gasteiger–Marsili formalism,[32] which is the type of atomic charges used in calibrating the AutoDock empirical free energy function.[31] Torsional degrees of freedom were defined with the help of AutoTors. A moderate torsion constraint was defined for the bond between the benzopyranone and the substituted phenyl ring in the flavone unit in order to avoid perpendicular conformations [i.e., a torsion angle of 90°; a perpendicular torsional barrier of about 3 kcal/mol has been reported for flavones].[33]

The crystal structure of the HIV-1 IN catalytic core domain obtained by Goldgur et al.[18] was used as protein structure. It was set up for docking as previously described.[19] The grid maps defining the search region and representing the protein in the actual docking process were calculated with AutoGrid and had dimensions of 30 Å×30 Å×30 Å, with a spacing of 0.375 Å between the grid points.

Acknowledgements

This work was supported by NIH grants GM56553 and AI34786 to F.D.B., the James B. Pendleton Charitable Trust and the Berger Foundation. F.D.B. is a Scholar of the Leukemia and Lymphoma Society of America. This work was further supported by NSF grant CHE-9807098 and NOAA/Sea Grant 2-MBT-N to W.F., and the molecular modeling was supported by NIH grant GM56553 to J.A.M. C.A.S. is grateful to the Austrian Science Fund for a postdoctoral fellowship (J1758-GEN). H.H.N is a NIH postdoctoral fellow under the training grant F32-GM63094-01. We thank MSI for the donation of the QUANTA and CHARMm software and Dr. Arthur Olson for the AutoDock program. We thank members of the Fenical and Bushman laboratories for suggestions and comments.

References and Notes

1. Hansen, M.; Carteau, S.; Hoffman, C.; Li, L.; Bushman, F. In *Genetic Engineering*; Setlow, J. K., Ed.; Plenum Press: New York, 1998; Vol. 20, pp 41–61.
2. Varmus, H.; Coffin, J. M.; Hughes, S. H. *Retroviruses*; Cold Spring Harbor Laboratory Press: Plainview, NY, 1997.
3. Hazuda, D. J.; Hastings, J. C.; Wolfe, A. L.; Emini, E. A. *Nuc. Acids Res.* **1994**, *22*, 1121.
4. Farnet, C. M.; Wang, B. B.; Lipford, J. R.; Bushman, F. D. *Proc. Nat. Acad. Sci. USA* **1996**, *93*, 9742.
5. Hazuda, D. J.; Felock, P.; Witmer, M.; Wolfe, A.; Stillmock, K.; Grobler, J. A.; Espeseth, A.; Gabryelski, L.; Schleif, W.; Blau, C.; Miller, M. D. *Science* **2000**, *287*, 646.
6. Wai, J. S.; Egbertson, M. S.; Payne, L. S.; Fisher, T. E.; Embrey, M. W.; Tran, L. O.; Melamed, J. Y.; Langford, H. M.; Guare, J. P.; Zhuang, L.; Grey, V. E.; Vacca, J. P.; Holloway, M. K.; Naylor-Olsen, A. M.; Hazuda, D. J.; Felock, P. J.; Wolfe, A. L.; Stillmock, K. A.; Schleif, W. A.; Gabryelski, L. J.; Young, S. D. *J. Med. Chem.* **2000**, *43*, 4923.
7. Pluymers, W.; Neamati, N.; Pannecouque, C.; Fikkert, V.; Marchand, C.; Burke, T. R.; Pommier, Y.; Schols, D.; De Clercq, E.; Debyser, Z.; Witvrouw, M. *Mol. Pharm* **2000**, *58*, 641.
8. Hwang, Y.; Rhodes, D.; Bushman, F. *Nuc. Acids Res.* **2000**, *28*, 4884.
9. Jensen, P. R.; Jenkins, K. M.; Porter, D.; Fenical, W. *Appl. Environ. Microbiol.* **1998**, *64*, 1490.
10. Bushman, F. D.; Craigie, R. *Proc. Nat. Acad. Sci. USA* **1991**, *88*, 1339.
11. Craigie, R.; Fujiwara, T.; Bushman, F. *Cell* **1990**, *62*, 829.
12. Katz, R. A.; Merkel, G.; Kulkosky, J.; Leis, J.; Skalka, A. M. *Cell* **1990**, *63*, 87.
13. Katzman, M.; Katz, R. A.; Skalka, A. M.; Leis, J. *J. Virol.* **1989**, *63*, 5319.
14. Kimpton, J.; Emerman, M. *J. Virol.* **1992**, *66*, 2232.
15. Hwang, Y.; Park, M.; Fischer, W. H.; Burgin, A.; Bushman, F. *Virology* **1999**, *262*, 479.
16. Engelman, A.; Craigie, R. *J. Virol.* **1992**, *66*, 6361.
17. Kulkosky, J.; Jones, K. S.; Katz, R. A.; Mack, J. P. G.; Skalka, A. M. *Mol. Cell Biol.* **1992**, *12*, 2331.
18. Goldgur, Y.; Craigie, R.; Cohen, G. H.; Fujiwara, T.; Yoshinaga, T.; Fujishita, T.; Sugimoto, H.; Endo, T.; Murai, H.; Davies, D. R. *Proc. Nat. Acad. Sci. USA* **1999**, *96*, 13040.
19. Sotriffer, C. A.; Ni, H.; McCammon, J. A. *J. Am. Chem. Soc.* **2000**, *122*, 6136.
20. Fesen, M. R.; Kohn, K. W.; Leteurtre, F.; Pommier, Y. *Proc. Nat. Acad. Sci. USA* **1993**, *90*, 2399.
21. Lafemina, R. L.; Graham, P. L.; Legrow, K.; Hastings, J. C.; Wolfe, A.; Young, S. D.; Emini, E. A.; Hazuda, D. J. *Antimicrob. Agents Chemother.* **1995**, *39*, 320.
22. Reddy, M. V. R.; Rao, M. R.; Rhodes, D.; Hansen, M. S. T.; Rubins, K.; Bushman, F. D.; Venkateswarlu, Y.; Faulkner, D. J. *J. Med. Chem.* **1999**, *42*, 1901.
23. Carteau, S.; Mouscadet, J. F.; Goulaouic, H.; Subra, F.; Auclair, C. *Arch. Biochem. Biophys.* **1993**, *305*, 606.
24. Nicklaus, M. C.; Neamati, N.; Hong, H. X.; Mazumder, A.; Sunder, S.; Chen, J.; Milne, G. W. A.; Pommier, Y. *J. Med. Chem.* **1997**, *40*, 920.
25. Hazuda, D.; Felock, P.; Hastings, J.; Pramanik, B.; Wolfe, A.; Goodarzi, G.; Vora, A.; Brackmann, K.; Grandgenett, D. *J. Virol.* **1997**, *71*, 807.
26. Fesen, M. R.; Pommier, Y.; Leteurtre, F.; Hiroguchi, S.; Yung, J.; Kohn, K. W. *Biochem. Pharmacol.* **1994**, *48*, 595.
27. Kim, H. J.; Woo, E. R.; Shin, C. G.; Park, H. *J. Nat. Prod.* **1998**, *61*, 145.
28. King, P. J.; Robinson, W. E. *J. Virol.* **1998**, *72*, 8420.
29. Bushman, F. D.; Engelman, A.; Palmer, I.; Wingfield, P.; Craigie, R. *Proc. Nat. Acad. Sci. USA* **1993**, *90*, 3428.
30. Charneau, P.; Clavel, F. *J. Virol.* **1991**, *65*, 2415.
31. Morris, G. M.; Goodsell, D. S.; Halliday, R. S.; Huey, R.; Hart, W. E.; Belew, R. K.; Olson, A. J. *J. Comput. Chem.* **1998**, *19*, 1639.
32. Gasteiger, J.; Marsili, M. *Tetrahedron* **1980**, *36*, 3219.
33. Meyer, M. *Int. J. Quantum Chem.* **2000**, *76*, 724.